ELSEVIER

A 3D-QSAR model for CYP2D6 inhibition in the aryloxypropanolamine series

Roy J. Vaz,*,† Akbar Nayeem, Kenneth Santone, Gamini Chandrasena and
Ashvinikumar V. Gavai*

Bristol-Myers Squibb Pharmaceutical Research Institute, PO Box 4000, Princeton, NJ 08543-4000, USA

Abstract—A comparative molecular similarity index analysis (CoMSiA) has been performed for cytochrome P450 2D6 inhibition on a series of aryloxypropanolamines to determine the factors contributing to this activity. The model is in agreement with a CYP2D6 homology model constructed on the basis of the mammalian CYP2C5 crystal structure. The energy minimized conformations were generated using the systematic search methodology in Sybyl 6.7. The model not only elucidated the relationship between structure and biological activity but, more importantly, provided useful strategies to modulate CYP2D6 affinity in the aryloxypropanolamine series.
© 2005 Elsevier Ltd. All rights reserved.

Cytochrome P450 2D6 (CYP2D6) has been reported as one of the primary metabolizing enzymes for compounds containing a basic amine.[1] Metabolism of compounds not containing a basic amine by CYP2D6 has also been reported.[2] CYP2D6 is absent in 5–9% of the Caucasian population, resulting in deficiencies in the oxidation of drugs that are metabolized primarily by this enzyme.[3] Due to the issues related to drug–drug interactions, as well as pharmacogenomic variability, small-molecule drug optimization involves optimizing compounds such that inhibitory activity towards CYP2D6 is minimized.[4,5] Common characteristics for inhibitors and substrates of CYP2D6 include a basic nitrogen atom, a hydrophobic region located 5–7 Å from the site of oxidation and hydrogen bonding elements.[6] Aryloxypropanolamines represent an important class of biologically active compounds that show potent inhibition of the CYP2D6 enzyme. This communication describes a CoMSiA[7] model for CYP2D6 inhibition for a series of analogues of propranolol. The model is in agreement with a docked model of the series into a CYP2D6 homology model constructed on the basis of the recently published[8] mammalian CYP2C5 crystal structure. The 3D-QSAR (CoMSiA) model was crucial in understanding the CYP2D6 structure–activity relationship in this series and provided strategies to design new analogues with reduced CYP2D6 inhibition.

Aryloxypropanolamines were found to be useful starting points in a study directed at certain G-protein coupled receptors. Propranolol (compound **7**) and analogues are known to be moderate inhibitors of CYP2D6 with IC$_{50}$ values in the low micromolar range (Table 1). However, analogues with an additional aromatic ring (such as compounds **5** and **13**) were found to have a significantly increased affinity for CYP2D6. The developed model was applied in design of analogues with decreased CYP2D6 inhibition.

To determine IC$_{50}$ values for CYP2D6, inhibition by the test substance of AMMC (3-[2-(N,N-diethyl-N-methylamino)ethyl]-7-methoxy-4-methylcoumarin) dealkylation was determined. Quinidine, an established inhibitor of CYP2D6, was used as the positive control. After buffer, cofactors, and test substance addition, the plates were pre-warmed to 37 °C. Incubations were initiated by the addition of pre-warmed enzyme (1.5 pmol cytochrome 450 recombinant human CYP2D6) and substrate (1.5 μmol). The final cofactor concentrations were 0.0081 mM NADP, 0.41 mM glucose-6-phosphate, and 0.4 U/mL glucose-6-phosphate dehydrogenase. The final incubation volume was 0.2 mL. At the end of the

R. J. Vaz et al. / Bioorg. Med. Chem. Lett. 15 (2005) 3816–3820

3817

Table 1. CYP2D6 IC$_{50}$ values for compounds in the CoMSiA model
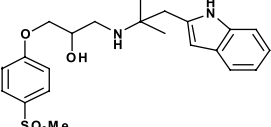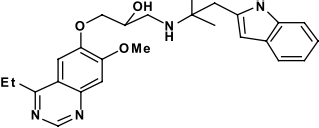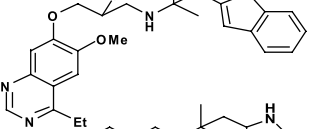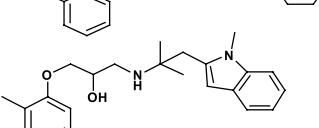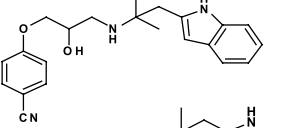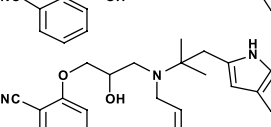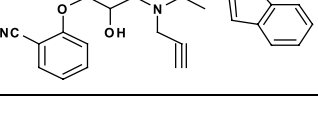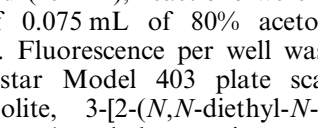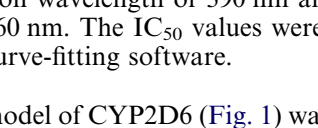
Compound No.	Structure	IC$_{50}$ (μM)
1		21
2		66
3		21
4		3.8
5		0.03
6		18
7		1.9
8		100
9		24
10		28
11		11
12		0.42
13		0.05
14		0.03

Table 1 (*continued*)

Compound No.	Structure	IC$_{50}$ (μM)
15		8.4
16		0.08
17		0.05
18		0.31
19		12
20		2.1
21		0.05
22		0.28
23		0.12
24		0.05
25		4.8
26		0.05
27		0.04

Table 1 (*continued*)

Compound No.	Structure	IC$_{50}$ (µM)
28		0.35
29		0.07
30		0.04
31		0.11
32		0.09
33		0.12
34		0.03
35		0.04
36		0.67

incubation period (45 min), reactions were stopped by the addition of 0.075 mL of 80% acetonitrile–20% 0.5 M Tris base. Fluorescence per well was measured using a FLUOstar Model 403 plate scanner. The AMMC metabolite, 3-[2-(*N,N*-diethyl-*N*-methylamino)ethyl]-7-hydroxy-4-methylcoumarin, was measured using an excitation wavelength of 390 nm and emission wavelength of 460 nm. The IC$_{50}$ values were calculated utilizing XLfit curve-fitting software.

The homology model of CYP2D6 (Fig. 1) was generated using COMPOSER within the SYBYL 6.7.1 suite, from the structure of CYP2C5 (PDB code 1DT6, 43% identity). Several low energy conformations of compound 13 were generated using the systematic search methodology in SYBYL 6.7 within 10 kcal/mol from the lowest energy conformation using the Tripos force field.

These structures were optimized using the MMFF94 force field as implemented in SYBYL. Conformations
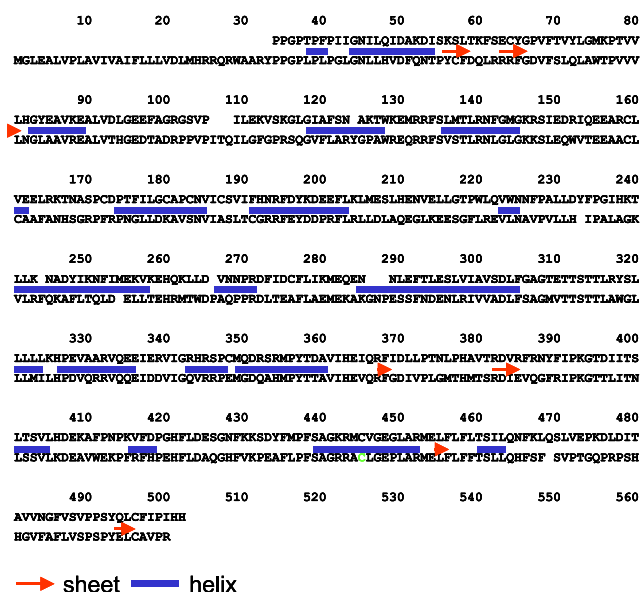

Figure 1. The alignment of CYP2D6 (lower sequence) with CYP2C5 secondary structure. The cysteine residue in green binds to the porphyrin.

within 5 kcal/mol from the minimum and those where the root-mean square distance (not including the H atoms) was greater than 2 Å from each other, were retained. The resulting four conformations were then docked into the homology model. Only the lowest energy U-shaped conformation shown in Figures 3 and 4 provided a good fit into the active site. Structures for the other compounds in Table 1 were generated using SYBYL from the docked conformation and optimized using the MMFF94 as implemented within SYBYL. The structures were then overlaid using the nitrogen, the neighboring hydrogen, and the oxygen of the ethanolamine functionality. This was the alignment used for the CoMSiA[3] as available within SYBYL. Compounds 4, 8, 11, 22, 25, and 28 were not used in the derivation of the CoMSiA but were used to check the predictive capability of the model. As shown in Figure 2, for the fitted versus actual plot, the predicted values fit within the standard errors of the fitted model. The CoMSiA fields were generated using the steric and the electrostatic probes. Inclusion of other CoMSiA fields did not improve the correlation. The default regions defined by SYBYL 6.7 were used together with a minimum sigma of 2.0. The steric field contributed 51% toward the QSAR.

The PLS results from the CoMSiA are shown in Figure 2 and the steric coefficient plots are shown in Figure 3 together with the docked structure of compound 13. The steric coefficient plots are shown as green contours for positive (0.03) and red contours for negative (−0.03) coefficients. The conformation of quinidine (Fig. 4) was generated using a searching technique similar to the one previously described for compound 13. The overlay of quinidine with compound 13 was done by a RMS-fit using the centroids of the benzene rings as defined, together with the amine nitrogen and the hydroxyl oxygen from both the molecules. This conformation of
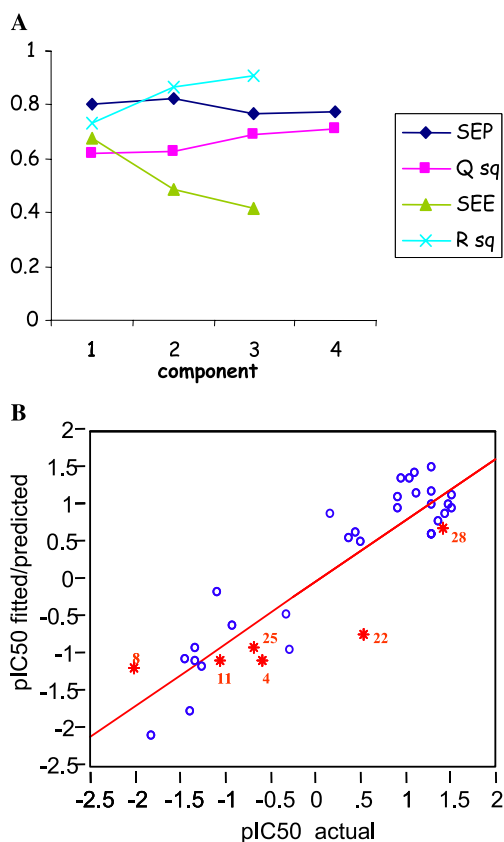
A

B

Figure 2. (A) Statistics from the PLS analysis and (B) fitted (blue), and predicted (red) versus actual pIC_{50} [log ($1/IC_{50}$) where IC_{50} is in μM] values using the CoMSiA model.

quinidine was overlaid on the conformation of compound **13** that had been docked into the homology model of CYP2D6.

The favorable statistics obtained from the CoMSiA model confirmed that these molecules adopt a U-shaped con-
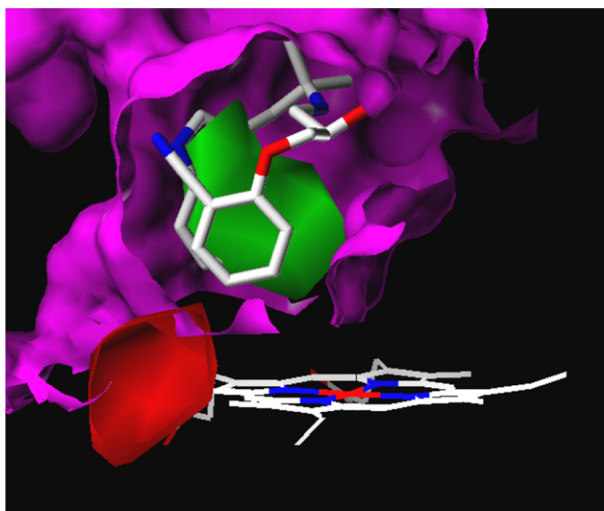

Figure 4. A model (orthographic projection) showing the indole group from compound **13** (magenta) and quinoline substitution at the quinuclidine nitrogen in quinidine occupying similar space. The overlay is in keeping with the reported SAR for analogues of quinidine.

formation. The conformation could be stabilized by a favorable π-stacking between the two aromatic rings. Figure 3 shows compound **13** docked into the homology model of CYP2D6. The red contour close to the heme group delineates the region where substitution creates sterically unfavorable interactions with either enzyme or cofactor in the active site. Substitution in this region should reduce affinity for the 2D6 enzyme. Indeed, appropriate substitution on either ring decreases CYP2D6 inhibitory potency (e.g., compounds **20** or **12** compared to **13**). The spatial arrangement shown in Figures 3 and 5 is in agreement with the structure of the observed metabolite (4-hydroxylation on the naphthalene group) upon CYP2D6-mediated oxidation of propranolol.[9]

The large hydrophobic pocket defined by the residues Phe120, Val370, Met374, Phe483, and Leu484, is shown in Figure 5. The basic nitrogen atom of the aryloxypropanolamine could potentially interact with Glu216[10] because the distance between the amine nitrogen and the carboxylate oxygen of Glu216 is around 4 Å. The

Figure 3. Compound **13** docked into the homology model of the enzyme. The coefficient plots from the CoMSiA model agree with the docked conformation. The reported metabolite pattern is also consistent with this mode.
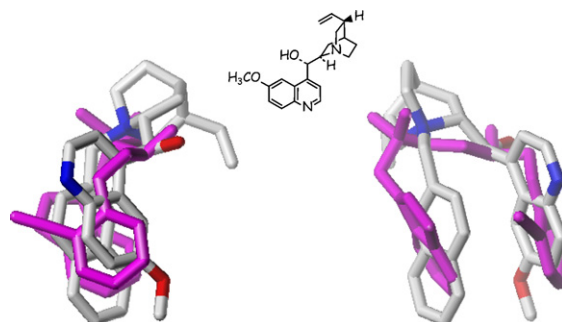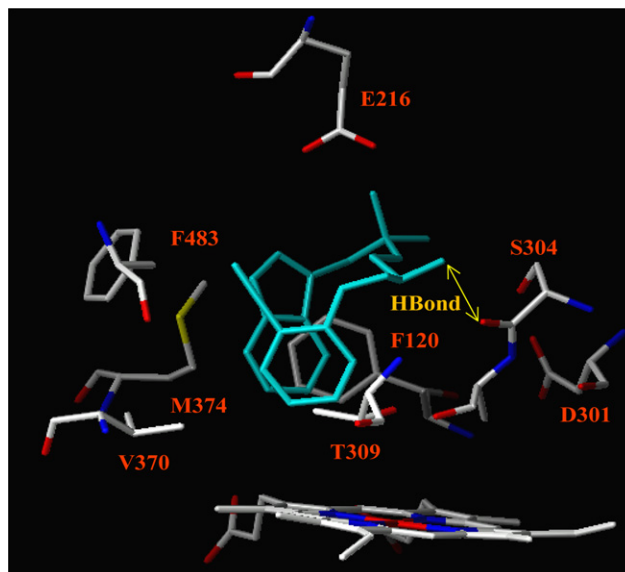

Figure 5. Residues that stabilize compound **13** in the active site of CYP2D6.

3820

R. J. Vaz et al. / Bioorg. Med. Chem. Lett. 15 (2005) 3816–3820

hydroxyl group may be involved in a hydrogen bond with the backbone carbonyl group of Ser304.

The overlay of quinidine on compound **13** (Fig. 4) shows agreement between the reported[11] structure–activity relationship for CYP2D6 inhibition by quinidine analogues and the aryloxypropanolamine SAR reported here. The CoMSiA model correctly predicts that substitution should be tolerated around the quinidine nitrogen atom. Figure 4 shows that such substitution would fall in the same space as that occupied by the indole group in compound **13**.

In summary, a combination of 3D-QSAR (CoMSiA) and a homology model based on CYP2C5 provided understanding of the optimal requirements for CYP2D6 affinity in the aryloxypropanolamine series. The model also suggested practical strategies to modulate CYP2D6 potency in this series.

Supplementary data

Supplementary data associated with this article can be found in the online version at doi:10.1016/j.bmcl.2005.06.007.

References and notes

1. Lewis, D. V. F.. In Gooderham, N., Ed.; Drug Metabolism: Towards the Next Millenium; IOS Press: The Netherlands, 1998, pp 1–12.
2. Guengerich, F. P.; Miller, G. P.; Hanna, I. H.; Martin, M. V.; Leger, S.; Black, C.; Chauret, N.; Silva, J. M.; Trimble, L. A.; Yergey, J. A.; Nicoll-Griffith, D. A. *Biochemistry* **2002**, *41*, 11025.
3. Essioux, L.; Destenaves, B.; Jais, P.; Thomas, F. In *Pharmacogenomics*; Licinio, J., Wong, M. L., Eds.; Wiley-VCH: Weinheim, 2002, pp 57–82.
4. Ashwell, M. A.; Lapierre, J.-M.; Kaplan, A.; Li, J.; Marr, C.; Yuan, J. *Bioorg. Med. Chem. Lett.* **2004**, *14*, 2025.
5. Biller, S. A.; Custer, L.; Dickinson, K. E.; Durham, S. K.; Gavai, A.; Hamann, L. G.; Josephs, J. L.; Moulin, F.; Pearl, G. M.; Flint, I. P.; Sanders, M.; Tymiak, A. A.; Vaz, R. In *Pharmaceutical Profiling in Drug Discovery for Lead Selection*; Borchardt, R. T., Kerns, E. H., Lipinski, C. A., Thakker, D. R., Wang, B., Eds.; AAPS Press: Arlington, VA, 2004; pp 413–429.
6. (a) Strobl, G. R.; von Kruedener, S.; Stockigt, J.; Guengerich, F. P.; Wolff, T. *J. Med. Chem.* **1993**, *36*, 1136; (b) de Groot, M. J.; Ackland, M. J.; Horne, V. A.; Alex, A. A.; Jones, B. C. *J. Med. Chem.* **1999**, *42*, 4062; (c) De Rienzo, F.; Fanelli, F.; Menziani, M. C.; De Benedetti, P. G. *J. Comp. Aided Mol. Des.* **2000**, *14*, 93.
7. (a) Klebe, G.; Abraham, U.; Mietzner, T. *J. Med. Chem.* **1994**, *37*, 4130; (b) Cramer, R. D., III; Patterson, D. E.; Bunce, J. D. *J. Am. Chem. Soc.* **1988**, *110*, 5959; (c) Cramer, R. D., III; DePriest, S. A.; Patterson, D. E.; Hecht, P. In *3D QSAR in Drug Design*; Kubinyi, H., Ed.; ESCOM: Leiden, 1993, pp 443–485; (d) Klebe, G. In Kubinyi, H., Ed.; 3D QSAR in Drug Design; Kluwer Academic: Great Britain, 1998; Vol. 3, pp 87–104.
8. Williams, P. A.; Cosme, J.; Sridhar, V.; Johnson, E. F.; McRee, D. E. *Mol. Cell* **2000**, *5*, 121.
9. Smith, D. A.; Jones, B. C. *Biochem. Pharmacol.* **1992**, *44*, 2089.
10. (a) Guengerich, F. P.; Miller, G. P.; Hanna, I. H.; Martin, M. V.; Leger, S.; Black, C.; Chauret, N.; Silva, J. M.; Trimble, L. A.; Yergey, J. A.; Nicoll-Griffith, D. A. *Biochemistry* **2002**, *41*, 11025; (b) Guengerich, F. P.; Hanna, I. H.; Martin, M. V.; Gillam, G. M. J. *Biochemistry* **2003**, *42*, 1245.
11. Hutzler, J. M.; Walker, G. S.; Wienkers, L. C. *Chem. Res. Toxicol.* **2003**, *16*, 450.